nature genetics

Dominant missense mutations in *ABCC9* cause Cantú syndrome

Magdalena Harakalova[1,18], Jeske J T van Harssel[1,18], Paulien A Terhal[1], Stef van Lieshout[1], Karen Duran[1], Ivo Renkens[1], David J Amor[2,3], Louise C Wilson[4], Edwin P Kirk[5], Claire L S Turner[6], Debbie Shears[7], Sixto Garcia-Minaur[8], Melissa M Lees[4], Alison Ross[9], Hanka Venselaar[10,11], Gert Vriend[10,11], Hiroki Takanari[12], Martin B Rook[12], Marcel A G van der Heyden[12], Folkert W Asselbergs[13], Hans M Breur[14], Marielle E Swinkels[1], Ingrid J Scurr[15], Sarah F Smithson[15], Nine V Knoers[1], Jasper J van der Smagt[1], Isaac J Nijman[1], Wigard P Kloosterman[1], Mieke M van Haelst[1,16], Gijs van Haaften[1] & Edwin Cuppen[1,17]

Cantú syndrome is characterized by congenital hypertrichosis, distinctive facial features, osteochondrodysplasia and cardiac defects. By using family-based exome sequencing, we identified a *de novo* mutation in *ABCC9*. Subsequently, we discovered novel dominant missense mutations in *ABCC9* in 14 of the 16 individuals with Cantú syndrome examined. The ABCC9 protein is part of an ATP-dependent potassium (K_{ATP}) channel that couples the metabolic state of a cell with its electrical activity. All mutations altered amino acids in or close to the transmembrane domains of ABCC9. Using electrophysiological measurements, we show that mutations in *ABCC9* reduce the ATP-mediated potassium channel inhibition, resulting in channel opening. Moreover, similarities between the phenotype of individuals with Cantú syndrome and side effects from the K_{ATP} channel agonist minoxidil indicate that the mutations in *ABCC9* result in channel opening. Given the availability of ABCC9 antagonists, our findings may have direct implications for the treatment of individuals with Cantú syndrome.

Cantú syndrome, also known as hypertrichotic osteochondrodysplasia (MIM 239850), is characterized by congenital hypertrichosis, distinctive facial features and cardiac defects[1]. The cardiac manifestations include patent ductus arteriosus, cardiomegaly, hypertrophy and pericardial effusion. Other clinical findings are macrosomia at birth, macrocephaly, deep palmar and plantar creases, recurrent upper and lower respiratory infections and skeletal dysplasia. On the basis of the first report of two affected siblings, the disorder was presumed to be an autosomal recessive disorder[1], but, in more recent studies, Cantú syndrome is clearly recognized as an autosomal dominant condition. Cantú syndrome is a rare disorder, with only 33 individuals with Cantú syndrome reported in the literature[1–12].

We performed exome sequencing in a child with Cantú syndrome and his unaffected parents. We tested for an autosomal *de novo* inheritance pattern by looking for heterozygous variant calls present in the child but absent in both parents. After mapping the raw sequencing reads against the reference genome (**Supplementary Table 1**) and applying variant calling filters, we identified 8,710 variants. After filtering against dbSNP132 and our in-house database and following application of a biological filter, five variants were considered for confirmation by Sanger sequencing in the child-parent trio. Out of these variants, a single *de novo* missense mutation in *ABCC9* was confirmed (**Supplementary Fig. 1**). The encoded p.Arg1154Gln variant is most likely damaging (predicted to be probably damaging, deleterious and deleterious by Polyphen-2, Condel and SIFT, respectively, using the Variant Effect Predictor tool (ENSEMBL version 67)) and highly conserved (Genomic Evolutionary Rate Profiling (GERP) scores of 4.33 (35 way)).

Next, we sequenced *ABCC9* in 15 additional Cantú syndrome cases, including 9 new and 6 previously published individuals with this syndrome (**Supplementary Table 2**). Sanger sequencing of the coding regions of *ABCC9* in these 15 individuals revealed 13 single

[1]Department of Medical Genetics, University Medical Center Utrecht, Utrecht, The Netherlands. [2]Murdoch Children's Research Institute, Royal Children's Hospital, Melbourne, Victoria, Australia. [3]Department of Paediatrics, University of Melbourne, Melbourne, Victoria, Australia. [4]Department of Clinical Genetics, Great Ormond Street Hospital, London, UK. [5]Department of Medical Genetics, Sydney Children's Hospital, Sydney, New South Wales, Australia. [6]Department of Clinical Genetics, Royal Devon and Exeter Hospital, Exeter, UK. [7]Clinical Genetics Department, Churchill Hospital, Oxford, UK. [8]Institute for Medical and Molecular Genetics, La Paz University Hospital, Madrid, Spain. [9]Department of Clinical Genetics, Foresterhill, Aberdeen, UK. [10]Center for Molecular and Biomolecular Informatics (CMBI), Nijmegen, The Netherlands. [11]Nijmegen Center for Molecular Life Sciences (NCMLS), Radboud University Nijmegen Medical Center, Nijmegen, The Netherlands. [12]Department of Medical Physiology, University Medical Center Utrecht, Utrecht, The Netherlands. [13]Department of Cardiology, Division of Heart and Lungs, University Medical Center Utrecht, Utrecht, The Netherlands. [14]Department of Pediatric Cardiology, University Medical Center Utrecht, Utrecht, The Netherlands. [15]Department of Clinical Genetics, St Michael's Hospital, Bristol, UK. [16]Section of Genomic Medicine, Imperial College London, London, UK. [17]Hubrecht Institute, The Royal Dutch Academy of Arts and Sciences, University Medical Center Utrecht, Utrecht, The Netherlands. [18]These authors contributed equally to this work. Correspondence should be addressed to E.C. (e.cuppen@hubrecht.eu) or G.v.H. (g.vanhaaften@umcutrecht.nl).

Received 26 January; accepted 14 May; published online 18 May 2012; corrected online 3 June 2012 (details online); doi:10.1038/ng.2324

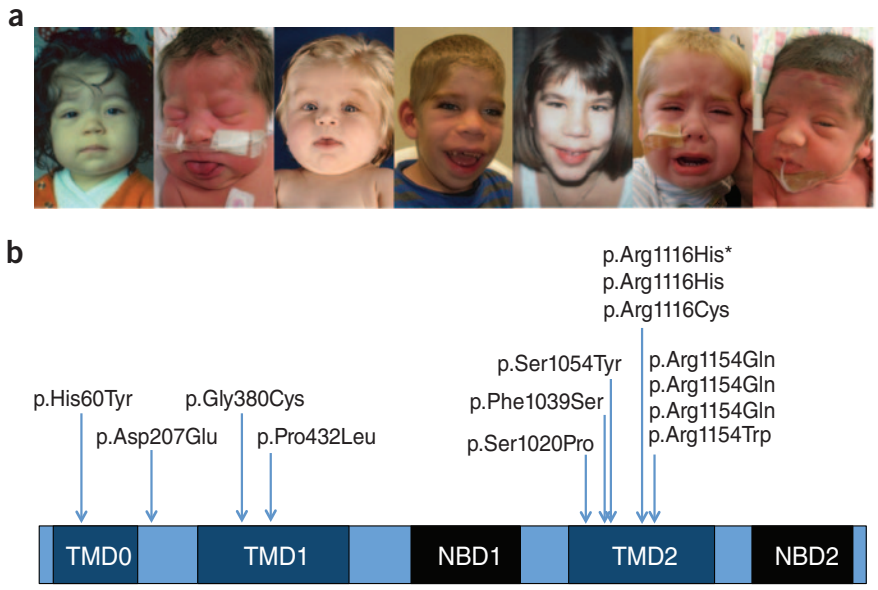

Figure 1 Clinical presentation of subjects with Cantú syndrome and mutations in *ABCC9*. (**a**) From left to right, pictures of subjects 3 (2 years), 4 (2 d), 5 (8 months), 7 (5 years), 8 (7 years), 10 (7 months) and 14 (1 d) at the indicated ages. Informed consent for publication of photographs was obtained from all subjects or their parents. (**b**) Schematic of ABCC9 protein structure including domains: TMD0, transmembrane domain 0, with five predicted transmembrane helices; TMD1, with six transmembrane helices; NBD1, nucleotide-binding domain 1; TMD2, with six transmembrane helices; and NBD2. All mutated residues are indicated. An asterisk indicates the variant that was present in the child of an affected mother.

heterozygous missense variants in *ABCC9* (Table 1), bringing the total number of variants identified in *ABCC9* to 14 in the 16 Cantú syndrome cases (**Fig. 1** and **Supplementary Table 2**). We were unable to find a variant in subjects 11 and 13, despite sequencing the full *ABCC9* ORF. Both subjects did not have cardiac phenotypes. Subject 11 had the most prominent and subject 13 the least prominent hair phenotype of all 16 individuals with Cantú syndrome included in this study (**Supplementary Note**). All variants affected highly conserved regions of the protein, and the majority are predicted to have a deleterious effect on protein function by several different prediction programs (**Supplementary Table 3**). None of these mutations were present in >5,000 publicly available whole-exome sequences (National Heart, Lung, and Blood Institute (NHLBI) Exome Sequencing Project (ESP)). For seven affected individuals, genetic material from both parents was available (**Supplementary Fig. 2**). Absence of the variant in both parents in these trios indicated that the variant arose in a *de novo* manner. In one male subject with Cantú syndrome, the mutation in *ABCC9* was inherited from an affected mother (**Supplementary Table 2**, subjects 2 and 3). Taken together, our findings show that Cantú syndrome is caused by dominant missense mutations in *ABCC9*.

ABCC9 (also known as *SUR2*) is located on human chromosome 12p12.1 and encodes a transmembrane protein of 1,549 amino acids. The ABCC9 protein is part of an ATP-sensitive potassium channel complex; a functional complex that consists of four subunits of a pore-forming potassium channel (KCNJ8 (also known as Kir6.1) or KCNJ11 (also known as Kir6.2)) and four regulatory ABCC9 subunits[13,14]. *ABCC9* is widely expressed, and two spliced forms with tissue-specific expression have been reported: *SUR2A* (expressed in cardiac and skeletal muscle) and *SUR2B* (expressed in vascular smooth muscle and hair follicles)[14,15]. The *ABCC9* splice variants differ only in their last exon. Heterozygous mutations in the exon unique to *SUR2A* have been linked to dilated cardiomyopathy[16] and atrial fibrillation[17]. All mutations identified in individuals with Cantú syndrome were located in more upstream exons and, hence, affect both spliced forms (**Fig. 1b**).

K_{ATP} channels are sensitive to intracellular ATP/Mg-ADP ratios and therefore couple the metabolic state of a cell to its electrical activity[18]. To gain insight into the effect of the mutations in *ABCC9*, we constructed a molecular model of the protein (**Fig. 2a**). The nucleotide-binding domains of ABCC9 are located intracellularly. Interaction between the Kir and SUR subunits takes place in both cytoplasmic and transmembrane regions[19]. Nucleotide binding is believed to result in conformational changes in the ABCC9 domains, resulting in opening of the potassium channel[20]. All mutations affected residues in or close to the transmembrane part of the protein, with the exception of the mutation affecting Asp207 (**Supplementary Table 4**). This residue is in the L0 loop, which is believed to directly interact with the potassium channel subunit[13]. The mutations appear to disturb the structure of the K_{ATP} channel complex. Notably, Pro432 is located in an α helix and forms only one of the two intrahelical hydrogen bonds, thus enabling kinking of the helix. The p.Pro432Leu alteration would render hinge-bending motion more difficult, thereby inhibiting conformational changes. A defect in one ABCC9 subunit out of the four present in a K_{ATP} complex is predicted to disturb channel functioning[21], thereby providing an explanation for the dominant effects observed in Cantú syndrome.

Table 1 Summary of detected heterozygous missense mutations in *ABCC9*

Subject	Chr.	Genomic alteration[a]	cDNA alteration	Protein alteration
9	12	g.22086822C>T	c.178C>T	p.His60Tyr
7	12	g.22068797C>A	c.621C>A	p.Asp207Glu
10	12	g.22063786G>T	c.1138G>T	p.Gly380Cys
5	12	g.22063116C>T	c.1295C>T	p.Pro432Leu
12	12	g.21998575T>C	c.3058T>C	p.Ser1020Pro
16	12	g.21997830T>C	c.3116>C	p.Phe1039Ser
15	12	g.21997785C>A	c.3161>A	p.Ser1054Tyr
2,3 (child and mother)	12	g.21995374G>A	c.3347G>A	p.Arg1116His
14	12	g.21995375C>T	c.3346C>T	p.Arg1116Cys
4	12	g.21995261C>T	c.3460C>T	p.Arg1154Trp
1,6,8	12	g.21995260G>A	c.3461G>A	p.Arg1154Gln

Chr., chromosome. None of the mutations were present in publicly available databases, including dbSNP135, the NHLBI Exome Sequencing Project (ESP) and our in-house database consisting of more than 60 exomes of Dutch origin.

[a]Genomic positions are based on Build GRCh37/hg19.

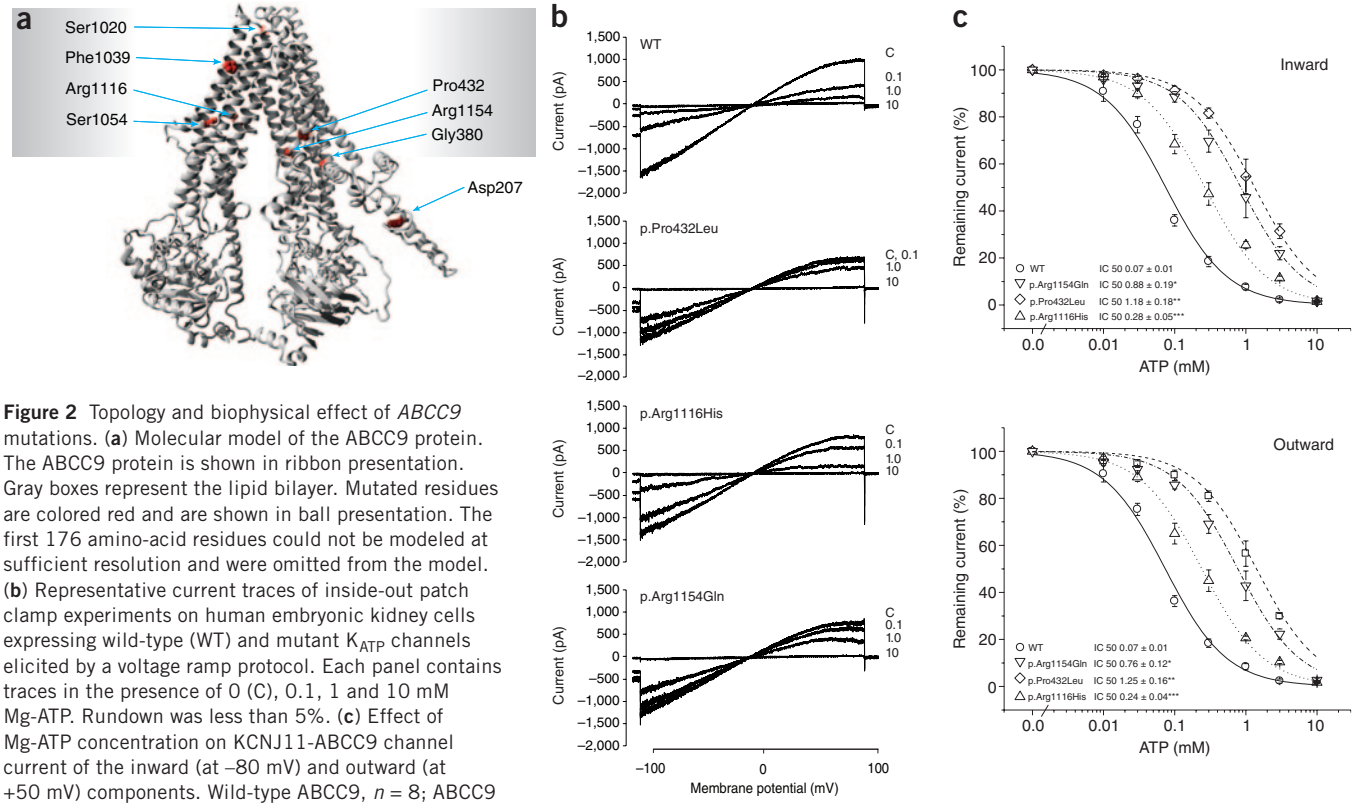

Figure 2 Topology and biophysical effect of *ABCC9* mutations. (**a**) Molecular model of the ABCC9 protein. The ABCC9 protein is shown in ribbon presentation. Gray boxes represent the lipid bilayer. Mutated residues are colored red and are shown in ball presentation. The first 176 amino-acid residues could not be modeled at sufficient resolution and were omitted from the model. (**b**) Representative current traces of inside-out patch clamp experiments on human embryonic kidney cells expressing wild-type (WT) and mutant K_{ATP} channels elicited by a voltage ramp protocol. Each panel contains traces in the presence of 0 (C), 0.1, 1 and 10 mM Mg-ATP. Rundown was less than 5%. (**c**) Effect of Mg-ATP concentration on KCNJ11-ABCC9 channel current of the inward (at –80 mV) and outward (at +50 mV) components. Wild-type ABCC9, $n = 8$; ABCC9 p.Arg1154Gln, $n = 7$; ABCC9 p.Pro432Leu, $n = 6$; ABCC9 p.Arg1116His, $n = 5$. Error bars, s.e.m. *, statistically significant differences in IC_{50} relative to wild-type protein ($P < 0.00001$, two-way ANOVA, Tukey's HSD *post hoc* test); **, statistically significant differences in IC_{50} relative to wild-type protein ($P < 0.00001$, two-way ANOVA, Tukey's HSD *post hoc* test); ***, statistically significant differences in IC_{50} relative to wild-type protein ($P = 0.004$, *t* test).

To study the effect of mutations in *ABCC9* on potassium channel function, we performed inside-out patch clamp experiments using human embryonic kidney cells co-expressing KCNJ11 and ABCC9, which results in a K_{ATP} channel makeup resembling that of ventricular channels. With expression of wild-type ABCC9, typical inward rectifier K_{ATP} (I_{KATP}) channel behavior was observed. Application of Mg-ATP inhibited I_{KATP} in a dose-dependent manner, with half-maximal inhibitory concentration (IC_{50}) values of 0.07 ± 0.01 (s.e.m.) mM for both inward and outward components (**Fig. 2b**,**c**). In contrast, ABCC9 p.Arg1154Gln (0.88 ± 0.19 and 0.76 ± 0.12 mM for inward and outward components, respectively), ABCC9 p.Pro432Leu (1.18 ± 0.18 and 1.25 ± 0.16 mM) and ABCC9 p.Arg1116His (0.28 ± 0.05 and 0.24 ± 0.04 mM) mutant channels showed reduced ATP sensitivity. For wild-type and all three mutant channels, complete blockade of activity was observed with 10 mM Mg-ATP. These results show that Cantú syndrome–related mutations in *ABCC9* reduce ATP-dependent inhibition of the I_{KATP} channel constituted by Kir6.2-SUR2A. In addition to aberrant regulation in the I_{KATP} subunit configuration tested, we expect that abnormal functioning of channels configured by other combinations of Kir6 and mutated SUR2 subunits will contribute to the wide variety and penetrance of Cantú syndrome characteristics.

An unexpected phenotypic overlap between individuals with Cantú syndrome and those treated with the drug minoxidil has been noted[9]. Minoxidil was developed as an antihypertensive vasodilator; however, potent side effects of hirsutism and pericardial effusions limited its use. Nowadays, the topical application of minoxidil is one of the most widely used treatments for male baldness. Minoxidil functions as a K_{ATP} channel agonist through direct binding to the ABCC9 subunit[22]. The similarities between the phenotypic characteristics of individuals with Cantú syndrome and the side effects of minoxidil treatment indicate that the mutations in *ABCC9* result in channel opening. In addition to agonists, several antagonists of K_{ATP} channels, such as glibenclamide and tolbutamide, have also been described. These channel blockers are used chronically for the treatment of diabetes. We believe that these observations may provide a starting point from which to develop new therapies to alleviate cardiac symptoms. Topical application of such blockers, under careful monitoring to exclude systemic absorption, may relieve the hair growth phenotypes in individuals with Cantú syndrome. Individuals with neonatal diabetes due to activating mutations in *ABCC8* (also known as *SUR1*) successfully switched from insulin treatment to treatment with an oral sulfonylurea (also a channel antagonist), showing that a mutated K_{ATP} channel can effectively be blocked in clinical practice[23].

In summary, we show that Cantú syndrome is caused by heterozygous missense mutations in *ABCC9*. Our electrophysiological experiments and the phenotypic overlap of individuals with Cantú syndrome and the side effects of minoxidil treatment indicate that the mutations result in dominant channel opening. Further studies are required to determine whether K_{ATP} channel antagonists can alleviate some of the symptoms of Cantú syndrome.

URLs. Integrative Genomics Viewer (IGV) browser for data visualization, http://www.broadinstitute.org/igv; Variant Effect Predictor, http://www.ensembl.org/tools.html; Exome Variant Server, NHLBI Exome Sequencing Project (ESP), http://evs.gs.washington.edu/EVS/; MAXC software, http://www.stanford.edu/~cpatton/downloads.htm; full description of modeling, http://www.cmbi.ru.nl/~hvensela/ABCC9/;

sequence data at Sequence Read Archive, http://www.ebi.ac.uk/ena/data/view/ERP001180.

METHODS

Methods and any associated references are available in the online version of the paper at http://www.nature.com/naturegenetics/.

Accession codes. Sequence data have been deposited at the European Molecular Biology Laboratory (EMBL)–European Bioinformatics Institute (EBI) Sequence Read Archive under accession ERP001180.

Note: Supplementary information is available on the Nature Genetics website.

ACKNOWLEDGMENTS

We thank the families of our subjects for participating in this study. We thank J.A. Sánchez-Chapula (Centro Universitario de Investigaciones Biomédicas de la Universidad de Colima) for providing wild-type KCNJ11 and ABCC9 expression constructs and N. Lansu and E. de Bruijn for technical support. F.W.A. is supported by a clinical fellowship from the Netherlands Organisation for Health Research and Development (ZonMw; 90700342). G.v.H. is supported by a Veni Grant from the Netherlands Organisation for Health Research and Development. This study was financially supported by the Child Health Priority Program of the University Medical Center Utrecht.

AUTHOR CONTRIBUTIONS

J.J.T.v.H., P.A.T., D.J.A., L.C.W., E.P.K., C.L.S.T., D.S., S.G.-M., M.M.L., A.R., F.W.A., H.M.B., M.E.S., I.J.S., S.F.S., J.J.v.d.S. and M.M.v.H. characterized individuals with Cantú syndrome and collected clinical data. M.H., K.D., I.R., W.P.K. and G.v.H. performed genetic studies, and M.H., S.v.L. and I.J.N. performed next-generation sequencing data analysis. H.V. and G.V. performed protein modeling studies. H.T., M.B.R. and M.A.G.v.d.H. designed and performed patch clamp experiments. G.v.H., M.H. and J.J.T.v.H. prepared the final manuscript. M.M.v.H., N.V.K., W.P.K., G.v.H. and E.C. supervised the study. All authors critically contributed to the study design and the manuscript.

COMPETING FINANCIAL INTERESTS

The authors declare no competing financial interests.

Published online at http://www.nature.com/doifinder/10.1038/ng.2324.
Reprints and permissions information is available online at http://www.nature.com/reprints/index.html.

1. Cantú, J.M., Garcia-Cruz, D., Sanchez-Corona, J., Hernandez, A. & Nazara, Z. A distinct osteochondrodysplasia with hypertrichosis—individualization of a probable autosomal recessive entity. *Hum. Genet.* **60**, 36–41 (1982).
2. Garcia-Cruz, D. *et al.* Congenital hypertrichosis, osteochondrodysplasia, and cardiomegaly: further delineation of a new genetic syndrome. *Am. J. Med. Genet.* **69**, 138–151 (1997).
3. Nevin, N.C., Mulholland, H.C. & Thomas, P.S. Congenital hypertrichosis, cardiomegaly and mild osteochondrodysplasia. *Am. J. Med. Genet.* **66**, 33–38 (1996).
4. Rosser, E.M. *et al.* Three patients with the osteochondrodysplasia and hypertrichosis syndrome—Cantú syndrome. *Clin. Dysmorphol.* **7**, 79–85 (1998).
5. Robertson, S.P. *et al.* Congenital hypertrichosis, osteochondrodysplasia, and cardiomegaly: Cantú syndrome. *Am. J. Med. Genet.* **85**, 395–402 (1999).
6. Concolino, D., Formicola, S., Camera, G. & Strisciuglio, P. Congenital hypertrichosis, cardiomegaly, and osteochondrodysplasia (Cantú syndrome): a new case with unusual radiological findings. *Am. J. Med. Genet.* **92**, 191–194 (2000).
7. Lazalde, B., Sanchez-Urbina, R., Nuno-Arana, I., Bitar, W.E. & de Lourdes Ramirez-Duenas, M. Autosomal dominant inheritance in Cantú syndrome (congenital hypertrichosis, osteochondrodysplasia, and cardiomegaly). *Am. J. Med. Genet.* **94**, 421–427 (2000).
8. Engels, H. *et al.* Further case of Cantú syndrome: exclusion of cryptic subtelomeric chromosome aberrations. *Am. J. Med. Genet.* **111**, 205–209 (2002).
9. Grange, D.K., Lorch, S.M., Cole, P.L. & Singh, G.K. Cantú syndrome in a woman and her two daughters: further confirmation of autosomal dominant inheritance and review of the cardiac manifestations. *Am. J. Med. Genet.* A. **140**, 1673–1680 (2006).
10. Tan, T.Y. *et al.* A patient with monosomy 1p36, atypical features and phenotypic similarities with Cantú syndrome. *Am. J. Med. Genet. A.* **139**, 216–220 (2005).
11. Scurr, I. *et al.* Cantú syndrome: report of nine new cases and expansion of the clinical phenotype. *Am. J. Med. Genet. A.* **155A**, 508–518 (2011).
12. Graziadio, C. *et al.* Short-term follow-up of a Brazilian patient with Cantú syndrome. *Am. J. Med. Genet. A.* **155A**, 1184–1188 (2011).
13. Babenko, A.P. & Bryan, J. SUR domains that associate with and gate K_{ATP} pores define a novel gatekeeper. *J. Biol. Chem.* **278**, 41577–41580 (2003).
14. Shi, N.Q., Ye, B. & Makielski, J.C. Function and distribution of the SUR isoforms and splice variants. *J. Mol. Cell. Cardiol.* **39**, 51–60 (2005).
15. Shorter, K., Farjo, N.P., Picksley, S.M. & Randall, V.A. Human hair follicles contain two forms of ATP-sensitive potassium channels, only one of which is sensitive to minoxidil. *FASEB J.* **22**, 1725–1736 (2008).
16. Bienengraeber, M. *et al. ABCC9* mutations identified in human dilated cardiomyopathy disrupt catalytic K_{ATP} channel gating. *Nat. Genet.* **36**, 382–387 (2004).
17. Olson, T.M. *et al.* K_{ATP} channel mutation confers risk for vein of Marshall adrenergic atrial fibrillation. *Nat. Clin. Pract. Cardiovasc. Med.* **4**, 110–116 (2007).
18. Flagg, T.P., Enkvetchakul, D., Koster, J.C. & Nichols, C.G. Muscle K_{ATP} channels: recent insights to energy sensing and myoprotection. *Physiol. Rev.* **90**, 799–829 (2010).
19. Mikhailov, M.V. *et al.* 3-D structural and functional characterization of the purified K_{ATP} channel complex Kir6.2–SUR1. *EMBO J.* **24**, 4166–4175 (2005).
20. Moreau, C., Prost, A.L., Derand, R. & Vivaudou, M. SUR, ABC proteins targeted by K_{ATP} channel openers. *J. Mol. Cell. Cardiol.* **38**, 951–963 (2005).
21. Nichols, C.G. K_{ATP} channels as molecular sensors of cellular metabolism. *Nature* **440**, 470–476 (2006).
22. Schwanstecher, M. *et al.* Potassium channel openers require ATP to bind to and act through sulfonylurea receptors. *EMBO J.* **17**, 5529–5535 (1998).
23. Rafiq, M. *et al.* Effective treatment with oral sulfonylureas in patients with diabetes due to sulfonylurea receptor 1 (SUR1) mutations. *Diabetes Care* **31**, 204–209 (2008).

ONLINE METHODS

Clinical samples. Informed consent for whole-exome sequencing as a part of the diagnostic process (approved by the Medical Ethical Committee of the University Medical Center Utrecht) was obtained for subject 1 and his parents. Informed consent for Sanger sequencing analysis was obtained for all subjects included in this study. Informed consent to publish clinical photographs was obtained for subjects 3, 4, 5, 7, 8, 10, 13 and 14 (**Fig. 1a** and **Supplementary Note**).

Multiplexed whole-exome next-generation trio sequencing. Genomic DNA was isolated from peripheral lymphocytes of subject 1 and his parents according to standard procedures. The concentration of genomic DNA was determined using Qubit Quant-iT (Invitrogen), and high-quality DNA (2 μg) from each member of the child-parent trio was used for the preparation of a barcoded fragment library, followed by multiplexed enrichment and sequencing on the SOLiD next-generation sequencing platform[24]. In brief, the DNA was fragmented using the Covaris S2 System (Applied Biosystems), yielding approximately 150-bp short fragments. After fragmentation, the DNA was end repaired and phosphorylated at the 5′ end using the End-It DNA End-Repair Kit (EpiCenter) and purified with the Agencourt AMPure XP system (Beckman Coulter Genomics). DNA was then ligated to double-stranded truncated adaptors compatible with the SOLiD next-generation sequencing platform using the Quick Ligation Kit (NEB). After purification, each sequencing library was nick translated, barcoded and amplified in a single PCR assay. The intensity of library bands was examined on a 2% agarose gel (Lonza FlashGel System). Amplified library fragments in the range of 175–225 bp in size were selected on a 4% agarose gel and purified using a QIAquick Gel Extraction Kit (Qiagen). Libraries from the child-parent trio were pooled in equimolar concentrations and were enriched using the Agilent SureSelect Human All Exon 50Mb Kit (Agilent Technologies). Enriched library pool fragments were amplified using 12 PCR cycles and elongated to a full-length adaptor sequence required for SOLiD sequencing. SOLiD sequencing was performed according to the instructions in the SOLiD 4 manual to produce enough 50-bp reads to obtain sufficient coverage for a single allele in each library. Sequencing and mapping statistics are summarized in **Supplementary Table 2**. Evenness scores were calculated as described[25].

Sequencing, variant detection and analysis. Raw sequencing reads were mapped against the human reference genome GRCh37/hg19 using our custom pipeline based on the Burrows-Wheeler Alignment (BWA) algorithm[26]. Sequence data were submitted to the EMBL-EBI Sequence Read Archive (see URLs). Single-nucleotide variants (SNVs) and small indels (≤7 nt) were called by our custom analysis pipeline as described[27] (all scripts are available upon request). The criteria for variant detection were set to enable discovery of *de novo* heterozygous variants. We required that variants should minimally be supported by two read seeds (first 25 bp, the higher quality portion of a read), and we set the cutoff for coverage to a minimum of ten reads and the cutoff for non-reference allele percentage to 15%. A maximum of five clonal reads (defined as reads with an identical start site) were included in the analysis. All common and rare polymorphisms present in Ensembl62 were flagged as known, and variants present in our in-house database (data from ~60 whole exomes) were considered to represent sequencing errors or Dutch population–specific variants; other variants were considered to be novel, consistent with an ultra-rare disease. For each variant, the genomic location, amino-acid change, effect on protein function, conservation score and output from prediction programs (Polyphen, Polyphen-2, SIFT and Condel) were collected and subsequently used for prioritization of the candidate variants.

Sanger sequencing validation. The coding sequences of *ABCC9*, *KCNJ8* and *KCNJ11* genes were sequenced using standard Sanger sequencing. Primer sequences are summarized in **Supplementary Table 5**.

Protein modeling. We built a homology model of ABCC9 using the experimentally solved structure of mouse mutlidrug resistance protein (Protein Data Bank (PDB) 3g5u). An automatic modeling script with standard parameters in the WHAT IF & YASARA Twinset was used for modeling. The identity between ABCC9 and the template was 20% over 1,363 residues. The percentage identity is very low, which means that the model provides an overview of the global structure of the protein but cannot be used for detailed mutation analysis. A detailed description of the protein modeling settings and results is provided (see URLS).

Patch clamping experiments. HEK293T cells cultured on glass coverslips were cotransfected with 0.5 μg of pcDNA-KIR6.2, 0.5 μg of pcDNA-SUR2A (wild type or mutant) and 0.25 μg of pEGFP1 expression constructs. Patch clamp measurements were performed using an AxoPatch 200B amplifier controlled by pClamp 9 software (Molecular Devices). Patch pipettes were made with a Sutter P-2000 puller (Sutter Instrument) and had resistances of 2–3 MΩ. Inside-out experiments were performed with a bath solution containing 131 mM KCl, 1 mM EGTA, 1 mM $MgCl_2$, 7.2 mM K_2HPO_4 and 2.8 mM KH_2PO_4 brought to pH 7.20 with KOH. The pipette solution contained 145 mM KCl, 1 mM $CaCl_2$, 1 mM $MgCl_2$ and 5 mM HEPES brought to pH 7.40 with KOH. To evaluate the ATP-dependent inhibition of wild-type and mutant IKir6.2-SUR2A channel currents, inside-out patch clamp measurements of IKir6.2-SUR2A activity were performed as described previously[28]. Excised membrane patches were placed close to the inflow region of the recording chamber. Currents were elicited using a ramp protocol, ranging from –100 to 100 mV in 5 s, starting from a holding potential of –40 mV. After recording control traces in bath solutions without Mg-ATP, excised membrane patches were exposed to bath solution containing 0.01, 0.03, 0.1, 0.3, 1, 3 or 10 mM Mg-ATP. The concentration of free Mg^{2+} (1 mM) and Mg-ATP were calculated with the MAXC standard program (see URLs). Fractional block of outward and inward current was calculated using current level at +50 mV and –80 mV, respectively, and values obtained with experimental solutions were normalized to corresponding values from the previously recorded control trace. The data obtained from each recording were fitted by Hill equation using Microcal Origin (ver.8, Microcal Software) to estimate IC_{50} values. Each data point is shown as mean ± s.e.m., and significance was estimated by one-way ANOVA test.

Nucleotide changes encoding the p.Arg1154Gln, p.Pro432Leu and p.Arg1116His alterations were engineered into the ABCC9 expression construct using the QuikChange II XL Site-Directed Mutagenesis Kit (Stratagene) and custom-designed mutagenesis primers. Sanger sequencing was performed to confirm the presence of introduced mutations (the sequences of all primers are available upon request).

24. Harakalova, M. *et al.* Multiplexed array-based and in-solution genomic enrichment for flexible and cost-effective targeted next-generation sequencing. *Nat. Protoc.* **6**, 1870–1886 (2011).
25. Mokry, M. *et al.* Accurate SNP and mutation detection by targeted custom microarray–based genomic enrichment of short-fragment sequencing libraries. *Nucleic Acids Res.* **38**, e116 (2010).
26. Li, H. & Durbin, R. Fast and accurate short read alignment with Burrows-Wheeler transform. *Bioinformatics* **25**, 1754–1760 (2009).
27. Nijman, I.J. *et al.* Mutation discovery by targeted genomic enrichment of multiplexed barcoded samples. *Nat. Methods* **7**, 913–915 (2010).
28. Ishihara, K. & Ehara, T. Two modes of polyamine block regulating the cardiac inward rectifier K^+ current I_{K1} as revealed by a study of the Kir2.1 channel expressed in a human cell line. *J. Physiol.* (Lond.) **556**, 61–78 (2004).